Experimental Studies and Analysis of the Vertical Emittance Growth in the ATF Extraction Line in 2007-2008

M. Alabau Pons, A. Faus-Golfe, P. Bambade, S. Kuroda,
G. White, M. Woodley, A. Scarfe

Experimental Studies and Analysis of the Vertical Emittance Growth in the ATF Extraction Line in 2007-2008

M. Alabau Pons[*][†], A. Faus-Golfe[*], P. Bambade[†‡]

S. Kuroda[‡], G. White[§], M. Woodley[§]

A. Scarfe[¶]

March 24, 2009

Abstract

The Extraction Line (EXT) of the Accelerator Test Facility (ATF) at KEK will transport the electron beam from the ATF Damping Ring (DR) to the future ATF2 Final Focus beam line. Since several years, the vertical beam emittance measured in the EXT line is significantly larger than that measured in the DR itself, and there are observations that the growth increases with beam intensity. A possible contribution is the non-linearity in the magnetic fields experienced by the beam when passing off-axis through several magnets shared by the DR and EXT beam line in the initial part of the extraction process. Tracking simulations including non-linear field errors in these magnets predict significant emittance growth when the beam is displaced vertically with respect to the nominal trajectory. An experimental program has been carried out during 2007-2008 to study the relation between the extraction trajectory and the anomalous emittance growth. This note reports on the results of this program.

[*]IFIC (CSIC-UV), Valencia, Spain
[†]LAL, Univ Paris-Sud, CNRS/IN2P3, Orsay, France
[‡]KEK, Tsukuba, Japan
[§]SLAC, Stanford, USA
[¶]Cockcroft Institute, Univ Manchester, UK

1 Introduction

The Accelerator Test Facility, ATF, is a Damping Ring (DR) built at KEK (Tsukuba, Japan) to demonstrate the production and measurement of the small emittance beams needed for future Linear Colliders. In 2008, a new project, ATF2, was completed in the extraction line of ATF. It consists of a scaled-down prototype version of the final focus sections planned in the ILC and CLIC linear collider designs. Its main goals are to establish several critical hardware and beam handling technologies needed to focus transverse electron beam sizes down to the required nanometer levels. At ATF2, the nominal vertical beam size will be about 37 nm for a vertical emittance of 12 pm at injection [1].

While small vertical emittances are consistently reproduced in the ATF DR [2], measurements of the extracted beam, performed in a dedicated diagnostics section located immediately downstream, have since many years given significantly larger values than expected [3]. This long-standing problem has motivated studies of several possible sources of emittance growth induced during extraction. One of these, arising from known non-linearities in the magnetic fields of a few magnets shared by the DR and extraction line at its very beginning, was investigated and found important [4].

Since this part of the extraction line has not been redesigned and remains essentially unchanged for ATF2, a more detailed evaluation of the impact of these non-linearites on the extracted vertical emittance was carried out, both computationally and experimentally, in order to devise a suitable mitigation plan.

In the next sections, after briefly recalling the computational analysis, the results of an extended experimental program carried out at KEK in 2007-2008 are reported.

2 Non-linear fields in the extraction region

To quantify the effect of non-linearities in the shared magnets involved in the extraction (QM6R, QM7R, BS1X, BS2X and BS3X, see Fig. 1), two-dimensional magnetic field computations were performed with the finite element code PRIAM [5], using explicit magnet geometries and parameters. The obtained field maps were fitted by polynomial functions in the complex plane to get continuous representations in the form of local multipole expansions. The results, summarized in [6], confirmed the earlier analysis [4] and showed that the largest effects arise from QM7R, where the main quadrupole gradient is reduced by a quarter compared to the nominal value, and where a significant sextupolar term is present.

Tracking simulations including these non-linear fields were then performed. They showed that the projected vertical emittance increases significantly when the beam passes off-axis vertically with respect to the reference trajectory in QM7R. The main effect comes from the $x - y$ coupling induced by the equivalent skew quadrupole which arises from the sextupolar term once the beam is vertically misaligned [7].
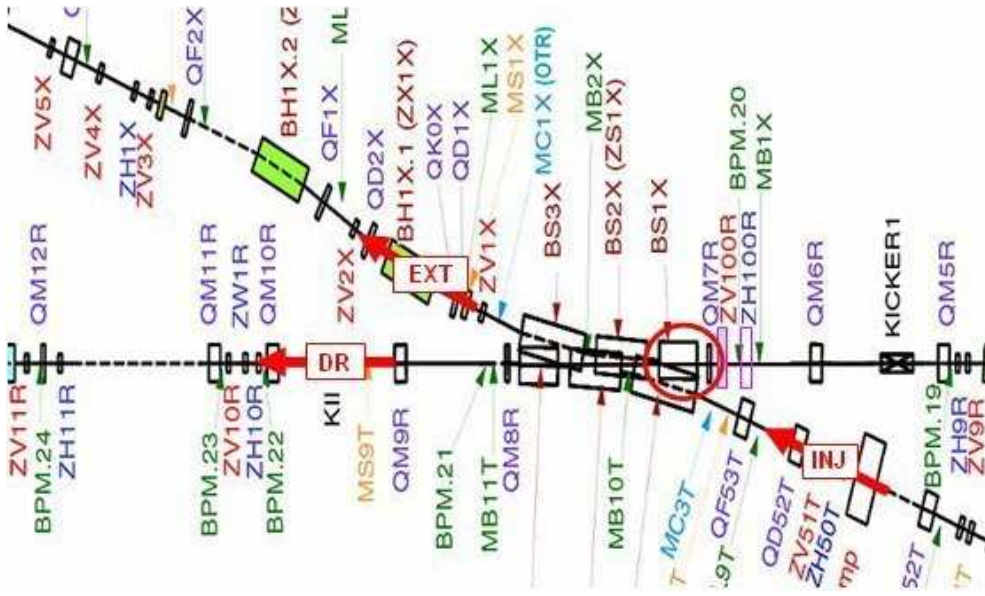
Figure 1: Schematic drawing of the extraction of the beam from ATF. The beam coming from the DR receives a first kick from the KICKER1, and then passes through two quadrupoles which are shared with the DR, QM6R and QM7R, and through three septum magnets, BS1X, BS2X and BS3X.

3 Overview of experimental program

To study the correlation between the emittance growth and orbit displacements in QM7R and to check the simulation results, an experimental investigation was carried out, which involved creating different vertical and horizontal orbits in QM7R by means of closed bumps in the DR, and measuring the projected vertical emittance downstream.

3.1 Local bump generation in QM7R

Vertical and horizontal trajectory offsets of varying amplitudes can be obtained in QM7R by means of closed bumps in the DR. The bumps can be opened in the DR by means of the ZV9R & ZV100R and ZH9R & ZH100R correctors and then closed with the ZV10R and ZH10R correctors, vertically and horizontally respectively. They can also be closed in the EXT line with ZV1X & ZV2X vertically and ZH1X & ZH2X horizontally. Details of corrector locations are shown in Fig.1.

3.2 Beam diagnostics

After the extraction region, there is a dispersion suppression section, ending with a second kicker which mirrors the initial one. The beam then goes through a horizontal dispersion-free zone, where five wire scanners are located for emittance measurements. Recent experience with such emittance measurements and reconstruction is described

in [8]. At the time of the experiments described in this report, the betatron phase advances between wire scanners could not be fully optimised to enable reliable emittance reconstruction. A complementary quadrupole scanning technique was also available, but because of practical constraints it could not be used easily during the shifts when trajectory bumps were applied.

An alternative method consisted in using an Optical Transition Radiation (OTR) monitor installed just after the septum magnets (see Fig. 1), at a location such that it imaged the beam angular spread out of QM7R with little influence from the beam size in QM7R, thus representing the growth in projected emittance from non-linearities in QM7R quite well. This allowed faster and more reliable results since the measured changes in vertical beam size at this location were well correlated with the emittance growth (see also the simulation study in [7]) and because the bumps did not need to be closed in the extraction line during the measurements.

Beam sizes at this location were recorded as a function of bump amplitudes in QM7R. In order to discriminate between a possible emittance growth due to the non-linear fields in the extraction and variations arising within the DR itself, measurements of stored beam sizes were simultaneously performed with the X-ray Synchrotron Radiation (XSR) monitor.

4 Summary of beam time periods in 2007-2008

Table 1 shows the beam time used in the different periods in 2007-2008 to measure beam sizes at the XSR and OTR monitors, in the DR and extraction line, respectively.

Shift	Date	Time
1	2007 December 19	9 PM to 10 PM
2	2008 March 4	1 AM to 9 AM
3	2008 May 14	5 PM to 1 AM (+1 day)
4	2008 May 22	5 AM to 5 PM
5	2008 May 28	9 AM to 1 AM (+1 day)

Table 1: Beam time used in 2007-2008 for simultaneous XSR and OTR vertical beam size measurements.

During each shift, after initial checks of the orbits and dispersion corrections, a vertical bump was set up in the DR to generate offsets in QM7R. Typical amplitudes which could be achieved within the maximum strengths of the steering correctors used were in the ±1 mm range. Beam intensities and digitized size information at the XSR and OTR monitors were then acquired for each bump setting.

Table 2 summarises the results obtained for minimum vertical beam sizes obtained during these scans and for the vertical emittances which could be infered from propagating the model β and dispersion functions. Simulated values are also shown for comparison, using DR measured emittances as input.

4

Beam conditions were different in the five data taking periods: while the measurements on the 19th of December 2007 and 28th of May gave values which could be compared with the simulation and interpreted in terms of coupling effects from QM7R, during the three other periods in March and May 2008, beam sizes at the OTR monitor were significantly larger and could not be explained in the context of the bump experiments subject of this report.

In the following sections, after summarising the conditions in each data taking period, the corresponding measurement and simulation results are presented, focusing the analysis on the data from the 19th of December 2007 and 28th of May.

	$\epsilon_{x,XSR}$ (nm·rad)	$\epsilon_{y,XSR}$ (pm·rad)	$\sigma_{y,OTR}$ (μm)		$\epsilon_{y,OTR}$ (pm·rad)	
			Measurement	Simulation	Measurement	Simulation
19 Dec'07	2.4	36.5	12.8	11.8	40	35
4 Mar'08	1.4	41.9	25.9	13.4	155	41
14 May'08	2.5	44.6	22.6	13.1	127	44
22 May'08	3.8	27.0	30.8	10.3	228	27
28 May'08	2.1	22.5	15.1	9.4	40	22

Table 2: Smallest vertical beam sizes measured at the OTR for the different vertical offsets implemented during successive shifts and corresponding emittances calculated from the β-function and dispersion obtained from the model. Vertical beam sizes and projected emittances at the OTR predicted from simulations using as input DR emittances obtained during the shifts. Horizontal and vertical emittances at the XSR monitor.

5 Simultaneous measurements at OTR and XSR beam size monitors

5.1 Measurements on the 19th of December 2007

The OTR monitor was installed in December 2007. On the 19th of December the first simultaneous OTR and XSR beam size measurements were done parasitically in a shift of another group, as a function of the vertical bump amplitude. The machine was already tuned and running in the one bunch per train, one train per pulse mode[1]. The beam intensity was relatively constant (see Fig. 2). The corrector strengths needed to create a 1 mm vertical bump amplitude in QM7R are shown in Table 3. Negative vertical bumps were generated in QM7R, in steps of 0.1 mm, down to a -0.8 mm amplitude. It was not possible to go to positive values because the strength of ZV9R was at its upper limit.

The raw OTR and XSR beam size data are shown in Fig. 3 top, in channels and μm, respectively. They are also shown after cuts to remove the data in between each stable setting of the bump, see Fig. 3 bottom, and after averaging, see Fig. 4, where the

---

[1]All measurements presented in this report were done with this mode of operation

error bars correspond to the standard deviation, the horizontal scale displays the bump amplitude and the vertical scale of the OTR measurements has been converted to μm by multiplying by a factor of 1.6^2.

In the range from 0.3 to 0.8 mm bump amplitude, the XSR beam size was relatively stable (see Fig. 4 right). The minimum beam size, and thus the minimum emittance configuration, may correspond to a non-zero bump amplitude if the beam has an initial offset. Here, the minimum OTR beam size was for a 0.3 mm bump amplitude (see Fig. 4 left), which can hence be considered as origin for the vertical displacements with respect to the center of QM7R. In Fig. 5 left, (blue line) the OTR measurements are shown with respect to this reference, in the restricted range where XSR beam sizes remained stable. Simulation results using as input DR emittances measured during the shift (green line) or nominal values (red line) are also shown.

The simulations tracked a Gaussian beam distribution of 50000 macro particles with energy 1.3 GeV and a flat energy distribution with 0.085% full width through the beam line, using an optical model representing the magnet settings during the shift and including the multipole coefficients computed in [6]. The vertical and horizontal DR emittances were computed from corresponding XSR beam sizes using the relation:

$$\epsilon_{y,x} = \sqrt{\sigma_{y,x}^2 - (\delta p/p \cdot D_{y,x})^2}/\beta_{y,x} \tag{1}$$

where the β-functions and dispersions were obtained from the on-line optical model of the DR (see Table 4).

Fig. 5 right shows the vertical emittances at the OTR computed from the same relation, using the measured beam sizes in Fig. 5 left and the vertical β-function and dispersion propagated to the OTR location using the model. Measured and simulated values for the minimum bump amplitude are also summarized in Table 4.

The simulation with nominal DR emittances (red line) and no bump gives much smaller OTR beam sizes than the measurement, while using the emittances determined during the shift (green line) improves the agreement. The growth when introducing the bump is however less than predicted by the simulation. Table 2 gives the minimum measured beam size and the corresponding value from the simulation[3].

To better account for the variations in the DR during the experiment, the ratio of both beam sizes was also studied (see Fig. 6 left), using in this case the full range of bump amplitudes. A second-order polynomial fit to this ratio gives:

$$f(y) = a(y - b)^2 + c = 0.78(y - 0.054)^2 + 1.39 \tag{2}$$

where the reduced χ^2=0.53, $f(y)$ is the ratio of the OTR and XSR beam sizes and y is the absolute bump amplitude. The minimum of the parabola corresponds to a bump amplitude of $y = 0.054$ mm. The rationale of fitting a second-order polynomial is because the main component in the QM7R multipolar field expansion [6] is a sextupole, and it

---

[2]The XSR data recorded already included the required calibration factor of 1.2.

[3]Small differences can be seen, which may due to differences between the optical model and the real machine. Such differences can also affect the conversion from measured beam sizes to emittances. Ideally, the β-function at the OTR location should be measured.

can be shown computing the transfer matrix that for a vertically displaced sextupole, the emittance squared has a quadratic dependance on the product of the displacement and corresponding strength [9].

Fig. 6 right shows the ratio of the OTR and XSR beam sizes, normalized to the minimum value, and in comparison with simulation predictions including the multipole coefficients computed in [6] for QM7R (blue lines) and for both QM7R and BS1X (magenta lines). Two cases are displayed, corresponding to the nominal extracted horizontal orbit of 22.5 mm in QM7R (blue crosses and magenta empty boxes) and to one displaced by about 1.5 mm towards the center of the quadrupole (blue cross-box and magenta full box). Since the magnet is more linear near its center, effects become smaller in this last case and the agreement with the measurements is improved.

ZV9R	1.94 A/mm
ZV100R	-1.56 A/mm
ZV10R	-1.42 A/mm

Table 3: Corrector strengths to create a closed bump in the DR with a 1 mm vertical amplitude in QM7R with the optics of the 19th of December 2007.
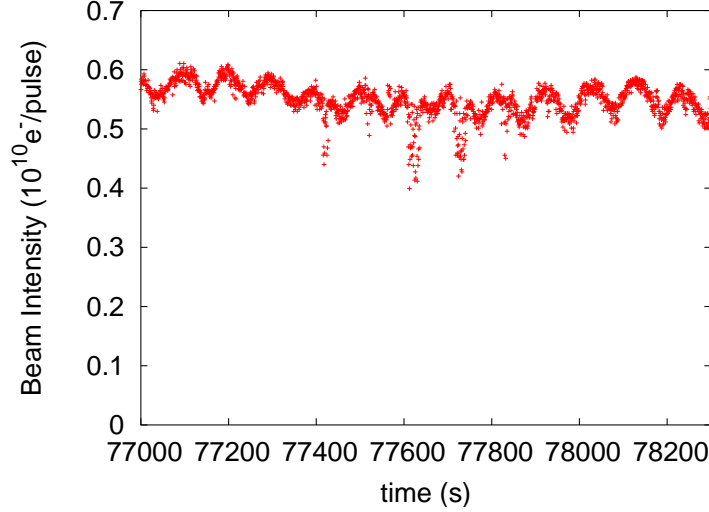

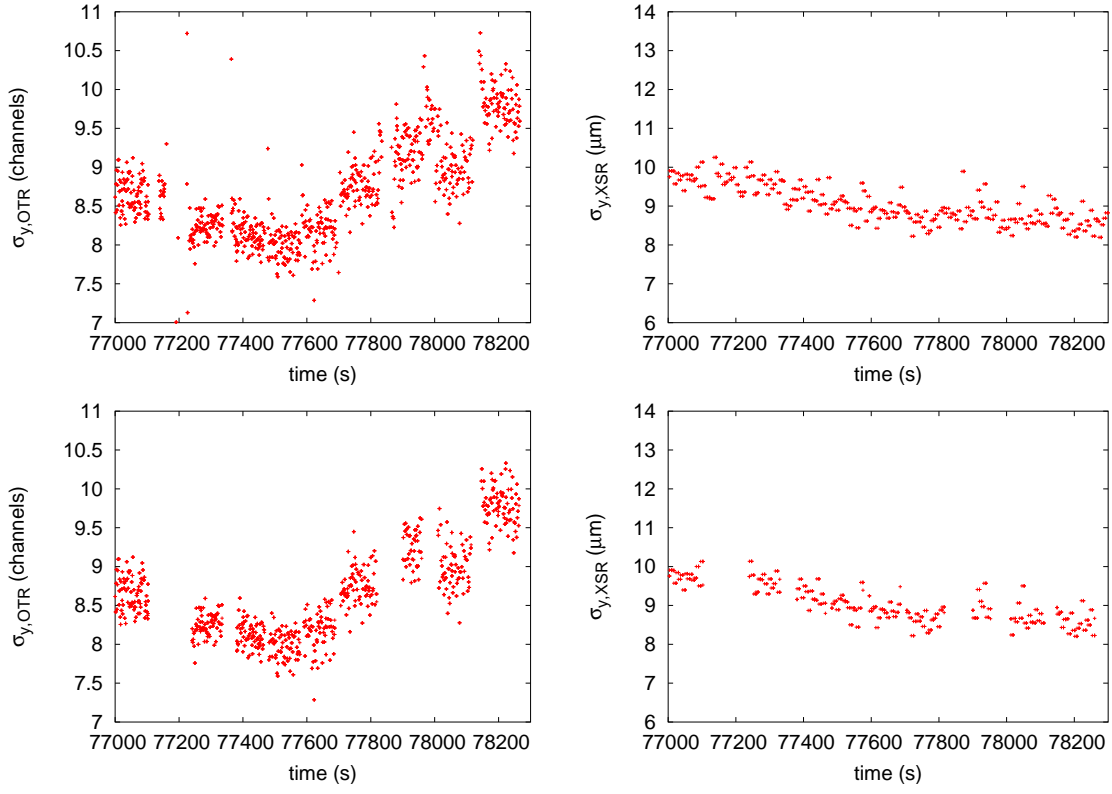Figure 2: Beam intensity during the beam size measurements on the 19th of December 2007.

Figure 3: Vertical beam sizes recorded at the OTR (left) and XSR (right) on the 19th of December 2007 as a function of time (top). Idem after removing data between each stable bump setting (bottom).
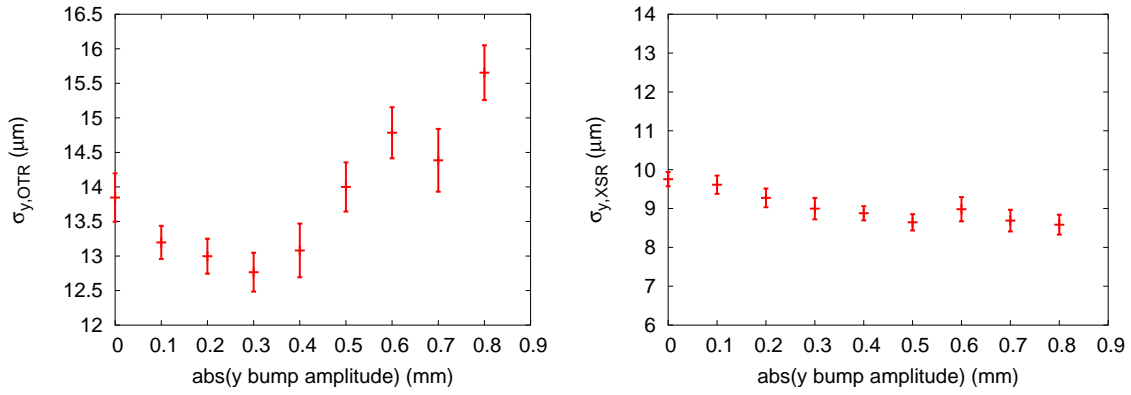

Figure 4: Vertical beam size at the OTR (left) and XSR (right) measured on the 19th of December 2007 as a function of the bump amplitude in QM7R.

XSR				OTR	
$\sigma_{y,meas}$ (μm)	9.0	$\sigma_{x,meas}$ (μm)	40.7	$\sigma_{y,meas}$ (μm)	12.8
β_y (m)	2.2	β_x (m)	0.5	$\beta_{x,y}$ (m)	10.6, 4.0
D_y (mm)	-0.4	D_x (mm)	23.4	D_y (mm)	2.9
ϵ_y (pm·rad)	36.5	ϵ_x (nm·rad)	2.4	ϵ_y (pm·rad)	39.6

Table 4: Emittances in the DR and at the OTR location during the shift of the 19th of December 2007, computed from the measured beam sizes and β-functions and dispersions at the XSR and OTR, obtained through an optical model of the DR and EXT line representing the settings of the magnets.
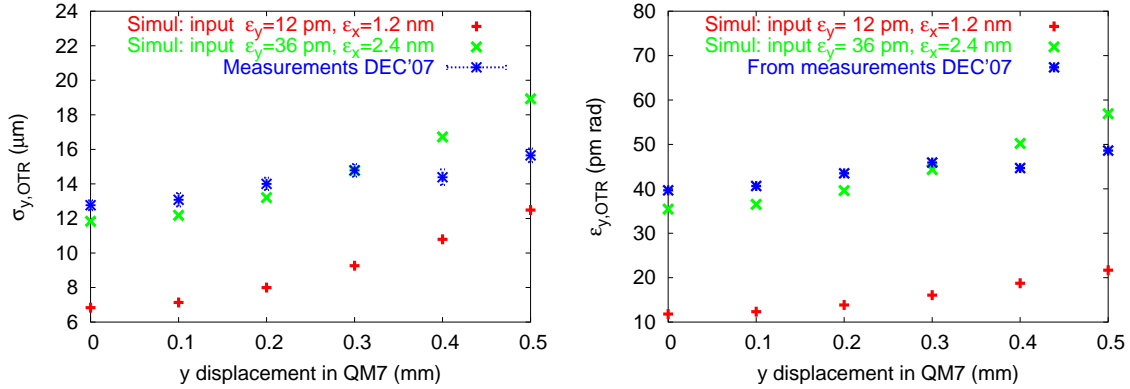
Figure 5: Vertical beam sizes at the OTR measured on the 19th of December 2007 (left) and corresponding emittances (right) as a function of vertical displacement in QM7R. Simulation results using as input DR emittances obtained from the magnetic configuration during the shift, or nominal values, are also shown.
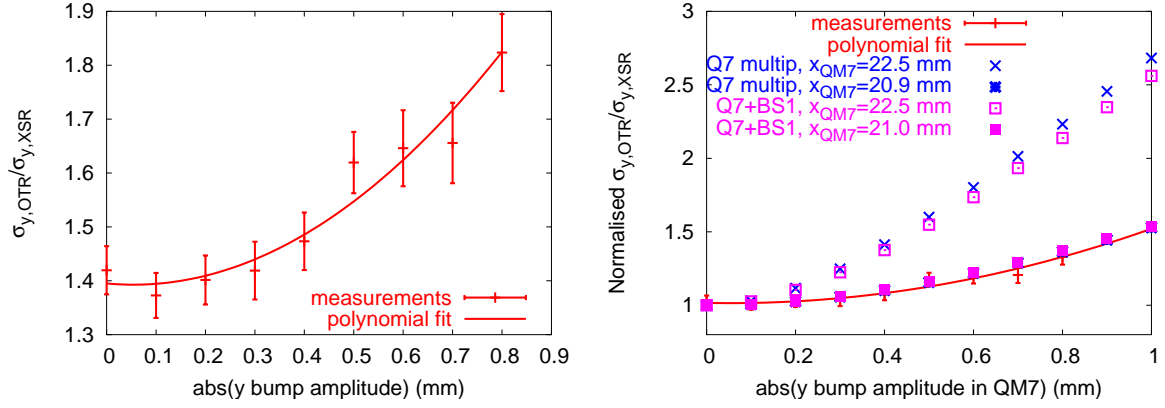
Figure 6: Ratio of vertical beam sizes at the OTR and XSR measured on the 19th of December 2007 (left) and ratio normalized to the minimum value (right), as a function of the vertical bump amplitude. In the graph on the right, tracking simulation results are also shown, including the computed non-linearities in QM7R and BS1X, for the nominal horizontal orbit in QM7R (22.5 mm) and for one closer to the center of the QM7R by 1.5 mm.

5.2 Measurements on the 4th of March 2008

During this shift, DR and EXT line orbit and dispersions were corrected[4]. The beam intensity during the shift was about 1×10^{10} electrons per pulse and experienced small variations (see Fig. 7). Beam sizes were recorded at the OTR and XSR as a function of a vertical bump in QM7R with amplitudes from 0 to 0.9 mm. The measurement was repeated twice about half an hour later (see Fig. 8). Since the three sets of data were fairly compatible, they were averaged (see Fig. 9). As can be seen, XSR beam sizes increased for large bump amplitudes, probably due to the fact that the bump was not perfectly closed in the DR. Some coupling between horizontal and vertical planes can in this case be induced through the sextupoles used for chromaticity correction in the DR. Fig. 10 shows the measurements at the OTR (blue line) and simulated values using as input the DR emittances from the shift (green line) and nominal values (red line). Emittances in the DR were computed from Eq. 1 using the measured beam sizes at the XSR and the β-functions and dispersions obtained from the on-line optical model (see Table 5). The vertical emittances were inferred from the beam sizes at the OTR using Eq. 1 and vertical β-function and dispersion values propagated to the OTR using the model. The values for the minimum bump amplitude are listed in Table 5.

As can be seen, measured beam sizes during the shift were two to three times bigger than can be explained with either nominal or measured input emittances in the DR. The emittances inferred at the OTR reach values as large as 155 pm·rad while in the DR it was only about 42 pm·rad (see Table 2). These anomalously large values could be due to anomalous dispersion, to a coupled beam coming from the DR, to a large horizontal displacement of the beam towards the external part of the QM7R magnet, where it is more non-linear [7], or to some other mechanism. Moreover, the relative increase at the XSR was about as large as at the OTR. There is not enough information from the measurements to explain the observations.

XSR				OTR	
$\sigma_{y,meas}$ (μm)	9.8	$\sigma_{x,meas}$ (μm)	33.9	$\sigma_{y,meas}$ (μm)	25.9
β_y (m)	2.3	β_x (m)	0.5	$\beta_{x,y}$ (m)	10.6, 4.3
D_y (mm)	0.18	D_x (mm)	23.4	D_y (mm)	0.3
ϵ_y (pm·rad)	41.9	ϵ_x (nm·rad)	1.38	ϵ_y (pm·rad)	155.4

Table 5: Emittances in the DR and at the OTR on the 4th of March 2008, computed from the measured beam sizes and modeled β-functions and dispersions at the XSR and OTR.

---

[4]Vertical dispersions need to be corrected down to less than about 10 mm in the diagnostic section to avoid biasing the emittance measurements.

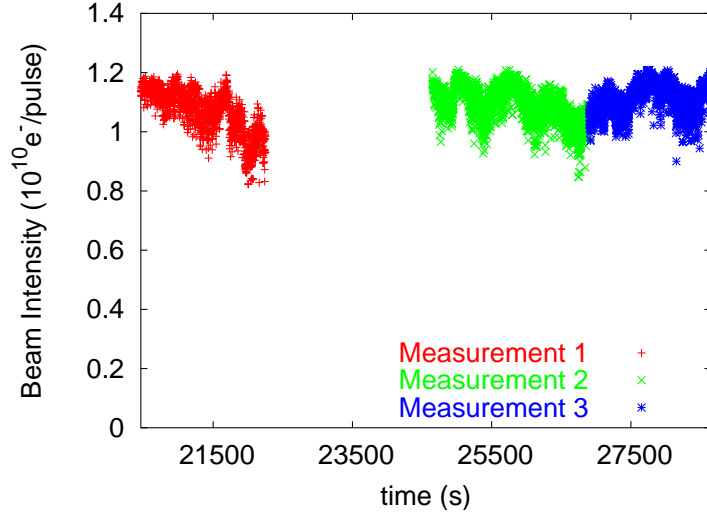Figure 7: Beam intensity during data taking on the 4th of March 2008.
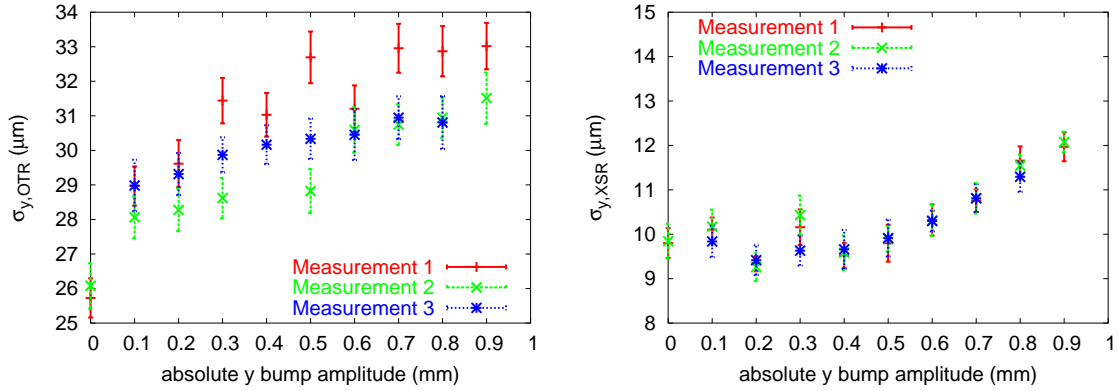

Figure 8: Vertical beam size at the OTR (left) and XSR (right) measured on the 4th of March 2008 as a function of the vertical bump amplitude in QM7R. Three series of measurements are shown.
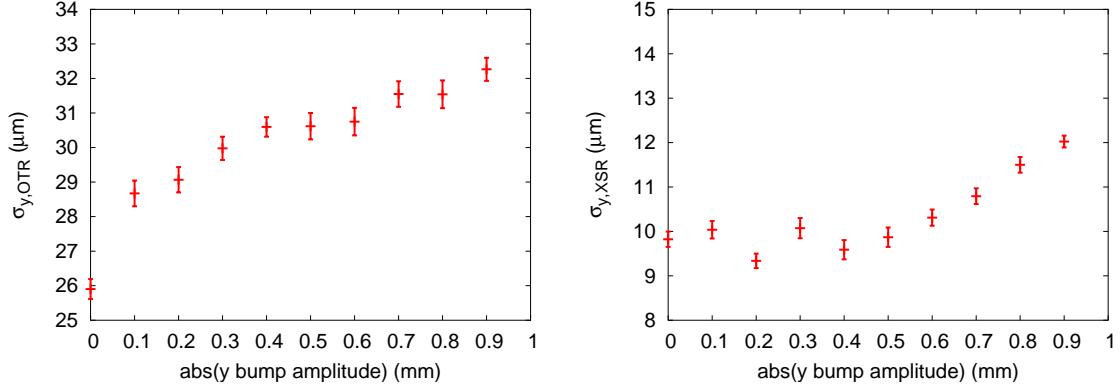
Figure 9: Average vertical beam size at the OTR (left) and XSR (right) measured on the 4th of March 2008 as a function of the bump amplitude in QM7R.
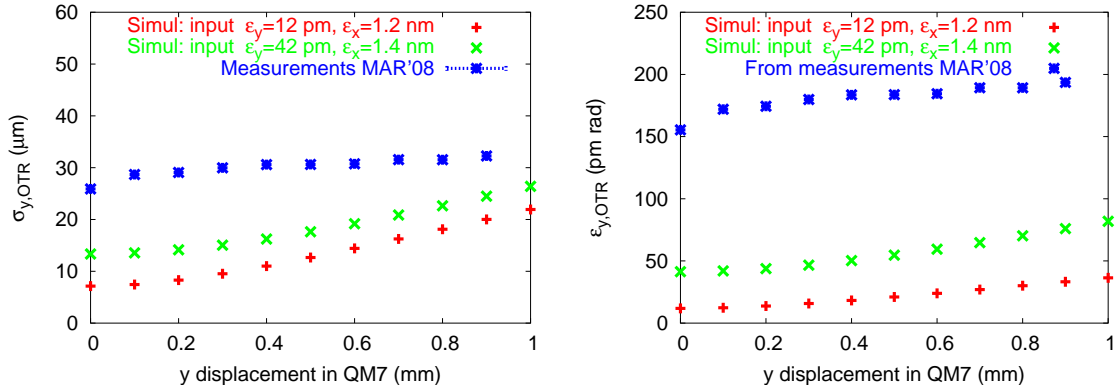

Figure 10: Vertical beam sizes (left) and emittances (right) measured at the OTR on the 4th of March 2008 as a function of the vertical displacement of the beam with respect to the center of QM7R. Beam sizes and emittances obtained from simulations using as input nominal and measured DR emittances are also shown.

13

5.3 Measurements on the 14th of May 2008

Measurements of OTR and XSR beam sizes with vertical bumps were also performed on the 14th of May 2008 in the range of amplitudes 0-0.6 mm (see Fig. 12). The intensity was about 0.55×10^{10} electrons per pulse but experienced some variations (see Fig. 11). As can be seen, the XSR beam size varied at least as much as the OTR one when applying the bump, probably due to the fact that, as in the shift on the 4th of March, the bump was not perfectly closed in the DR, causing some coupling between horizontal and vertical planes through the sextupoles.

The vertical and horizontal DR emittances computed during the shift from beam sizes measured at the XSR location are shown in Table 6. In addition to using the optical functions from the model as in previous shifts, explicit measurements of the β-function at the XSR location were performed by scanning DR quadrupoles and recording tune shifts. Simulation results for the OTR beam size using these DR emittances as input were obtained and are shown in Table 2, together with the smallest measured value, corresponding to a -0.4 mm bump. As in the shift on 4th of March, the measurement gave much larger values than the prediction and there is not enough information to determine the cause.
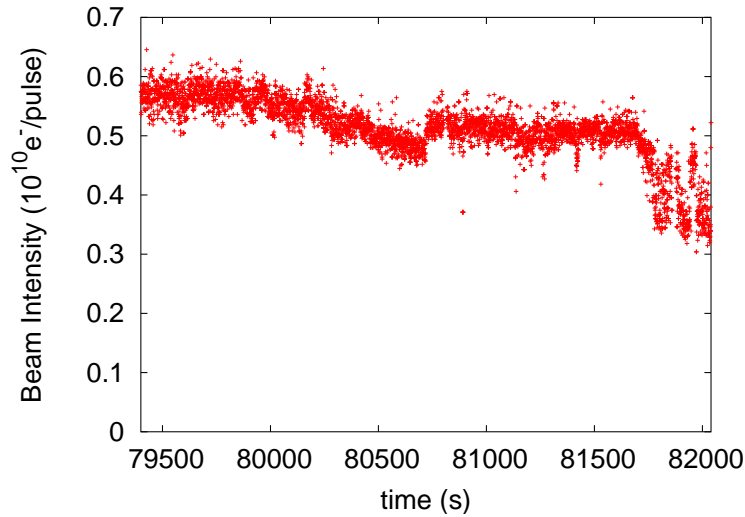

Figure 11: Beam intensity during data taking on the 14th of May 2008.
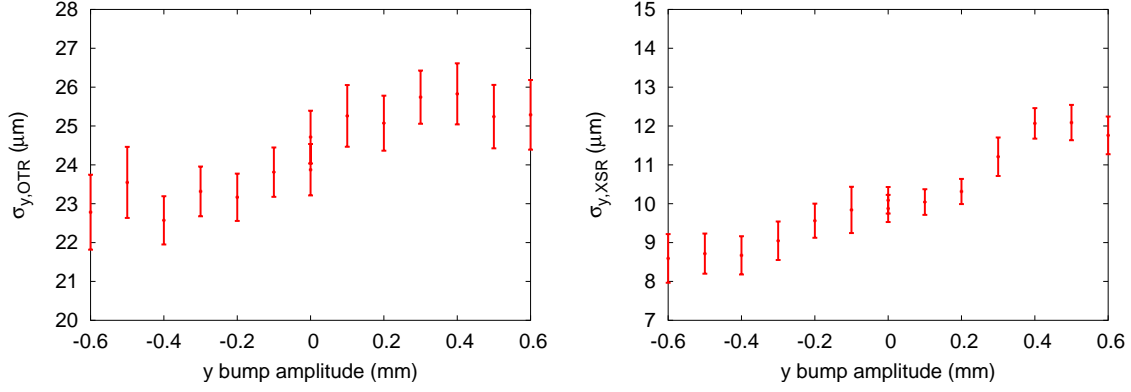
14

Figure 12: Vertical beam size at the OTR (left) and XSR (right) measured on the 14th of May 2008 as a function of the absolute vertical bump amplitude in QM7R.

XSR				OTR	
$\sigma_{y,meas}$ (μm)	9.9	$\sigma_{x,meas}$ (μm)	41.3	$\sigma_{y,meas}$ (μm)	22.6
$\beta_{y,model}$ (m)	2.2	$\beta_{x,model}$ (m)	0.5	$\beta_{x,y}$ (m)	10.8, 3.9
$D_{y,model}$ (mm)	-0.3	$D_{x,model}$ (mm)	23.3	D_y (mm)	-3.9
$\epsilon_{y,model}$ (pm·rad)	44.6	$\epsilon_{x,model}$ (nm·rad)	2.48	ϵ_y (pm·rad)	127.1
$\beta_{y,meas}$ (m)	2.9				
$\epsilon_{y,meas}$ (pm·rad)	33.6				

Table 6: Emittances in the DR and at the OTR on the 14th of May 2008, computed from the measured beam sizes and modeled β-functions and dispersions at the XSR and OTR. The vertical β-function measured at the XSR location during the shift and the corresponding emittance are also shown.

5.4 Measurements on the 22nd of May 2008

Measurements of OTR and XSR beam sizes with vertical bumps were also performed on the 22th of May 2008 in the range of amplitudes 0-0.8 mm (see Fig. 14). This time, the image of the beam at the OTR monitor was tilted (unlike the profile at the XSR monitor), and the beam was oscillating from left to right, probably due to some energy jitter. The intensity was not very stable (see Fig. 13), and the linac had to be retuned at some point to recover acceptable injection efficiency when it got below 0.2×10^{10} electrons per pulse. Again, the measured OTR beam sizes were much larger than could be explained by simulating using measured DR emittances as input (see Table 7 and Table 2).
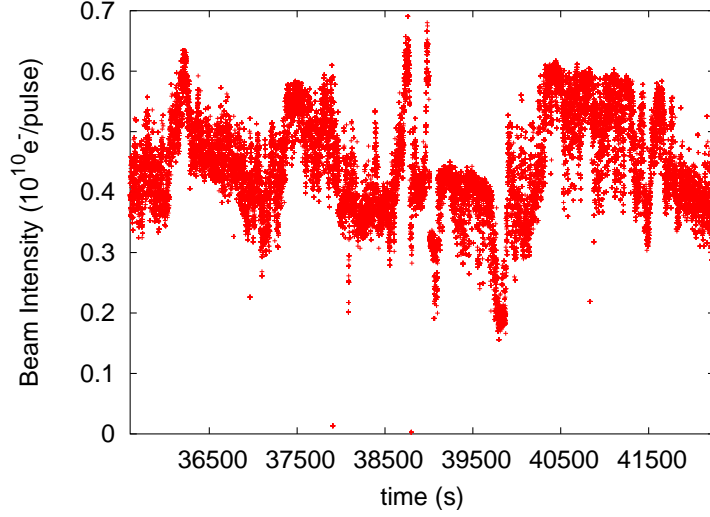

Figure 13: Beam intensity during data taking on the 22th of May 2008.
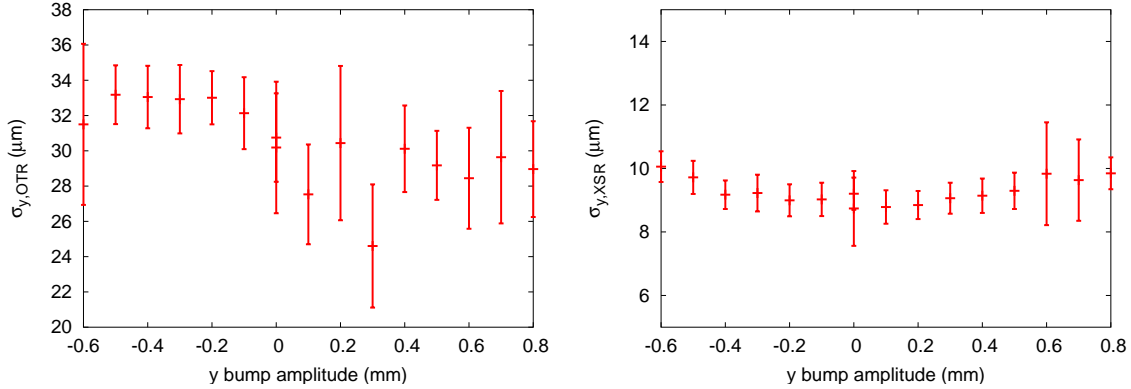

Figure 14: Vertical beam size at the OTR (left) and XSR (right) measured on the 22th of May 2008 as a function of the vertical bump amplitude in QM7R.

16

XSR				OTR	
$\sigma_{y,meas}$ (μm)	8.7	$\sigma_{x,meas}$ (μm)	48.7	$\sigma_{y,meas}$ (μm)	30.8
$\beta_{y,model}$ (m)	2.2	$\beta_{x,model}$ (m)	0.5	$\beta_{x,y}$ (m)	10.6, 3.9
$D_{y,model}$ (mm)	4.9	$D_{x,model}$ (mm)	23.3	D_y (mm)	8.0
$\epsilon_{y,model}$ (pm·rad)	27.0	$\epsilon_{x,model}$ (nm·rad)	3.83	ϵ_y (pm·rad)	228.0
$\beta_{y,meas}$ (m)	3.3				
$\epsilon_{y,meas}$ (pm·rad)	17.8				

Table 7: Emittances in the DR and at the OTR on the 22th of May 2008, computed from the measured beam sizes and modeled β-functions and dispersions at the XSR and OTR. The vertical β-function measured at the XSR location during the shift and the corresponding emittance are also shown.

5.5 Measurements on the 28th of May 2008

Measurements of OTR and XSR beam sizes with vertical bumps were repeated on the 28th of May 2008 in the range -1 to +1 mm. The beam intensity was not recorded, but it was checked for each measurement that it remained reasonably unchanged, with about 0.6×10^{10} electrons per pulse. Fig. 15 shows the results at the OTR (right) and XSR (left) monitors as a function of the vertical bump amplitude.

Fig. 16 shows the comparison of the measurements (blue line) with the simulation, including multipoles in QM7R and using DR emittances determined during the shift (see Table 8). Two input conditions were considered for the transverse phase space extracted from the DR, either with (green line) or without (red line) the presence of $x - y$ coupling[5]. The measurement at the OTR for a zero amplitude bump was bigger than predicted by simulating with an uncoupled input beam. Using a coupled input beam, it did get closer but still remained smaller than the measurement. In this case, the dependance on bump amplitude became rapidly stronger, indicating that the coupling effects introduced into the simulation of the input phase space may have been too large. The vertical emittance at the OTR was computed from the measured beam size and modeled vertical β-function and dispersion. Values for the minimum of the measurement, corresponding to an amplitude of 0.5 mm, are listed in Table 8.

To take into account the variations of the DR beam size during the experiment (see Fig. 15 right), the ratio of OTR and XSR beam sizes was studied (see Fig. 17 left) as for the data taken on the 19th of December. Fitting a second-order polynomial gives in this case:

$$f(y) = a(y - b)^2 + c = 0.19(y - 0.76)^2 + 1.62 \tag{3}$$

where the reduced $\chi^2 = 0.70$ and the minimum corresponds to a bump amplitude of $y = 0.76$ mm.

Fig. 17 right shows the ratio of the OTR and XSR beam sizes, normalized to the minimum value, and in comparison with simulation predictions including the multipole coefficients computed in [6] for QM7R (blue lines) and for both QM7R and BS1X (magenta lines). As for the data taken on the 19th of December, two cases are displayed, corresponding to the nominal extracted horizontal orbit of 22.5 mm in QM7R (blue crosses and magenta empty boxes) and to one displaced towards the center of the quadrupole (blue cross-box and magenta full box), where it is more linear and effects can be expected to be less. For the data taken on the 28th of May, since the measured emittance growth was weaker than on the 19th of December, a larger horizontal displacement is needed to explain the data. As can be seen in Fig. 17 right, a reasonable agreement is found for a 2.7 mm offset compared to 1.5 mm on December 19, 2007.

---

[5]The skew quadrupoles in the DR were turned on during the measurements as part of the standard coupling correction procedure. Although the residual coupling in the DR results both from these skew quads and the misalignments and errors which they should correct, taking them into account in the simulation of the phase space of the extracted beam can give a representative estimate of the correlations between the horizontal and vertical coordinates. This was done to simulate the presence of $x - y$ coupling effects.
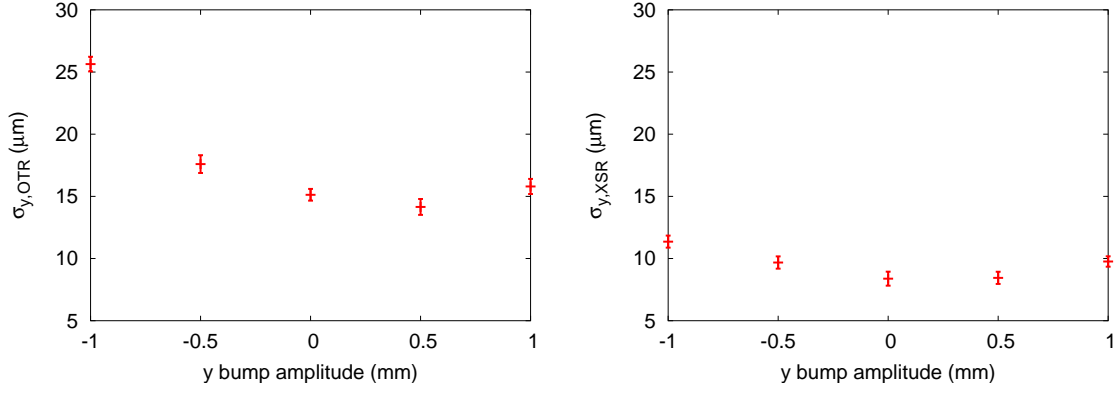
Figure 15: Vertical beam size at the OTR (left) and XSR (right) measured on the 28th of May 2008 as a function of the vertical bump amplitude in QM7R.
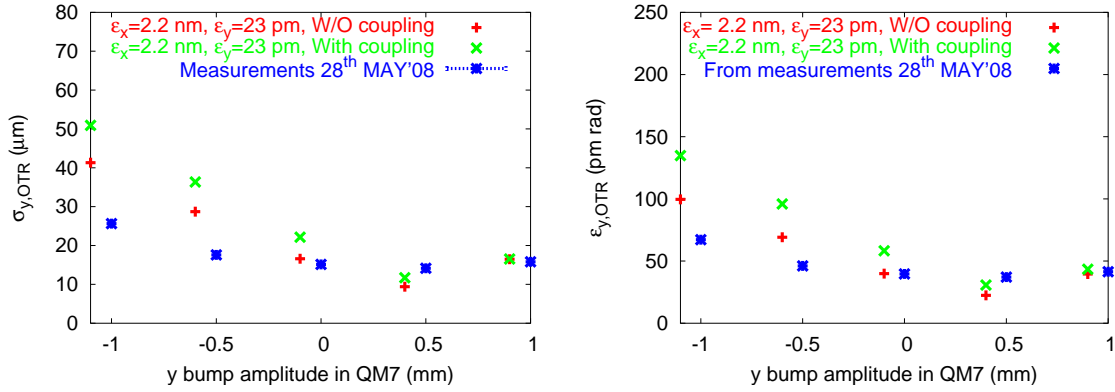

Figure 16: Vertical beam sizes at the OTR measured on the 28th of May 2008 (left) and corresponding emittances (right) as a function of vertical displacement in QM7R. Simulation results using as input DR emittances obtained from the magnetic configuration during the shift, or nominal values, are also shown.

XSR				OTR	
$\sigma_{y,meas}$ (μm)	8.4	$\sigma_{x,meas}$ (μm)	38.6	$\sigma_{y,meas}$ (μm)	14.2
β_y (m)	2.2	β_x (m)	0.5	$\beta_{x,y}$ (m)	10.1, 3.9
D_y (mm)	5.4	D_x (mm)	23.3	D_y (mm)	7.4
ϵ_y (pm·rad)	22.5	ϵ_x (nm·rad)	2.14	ϵ_y (pm·rad)	37.1

Table 8: Emittances in the DR and at the OTR location during the shift of the 28th of May 2008, computed from the measured beam sizes and β-functions and dispersions at the XSR and OTR obtained through an optical model of the DR and EXT line representing the settings of the magnets.
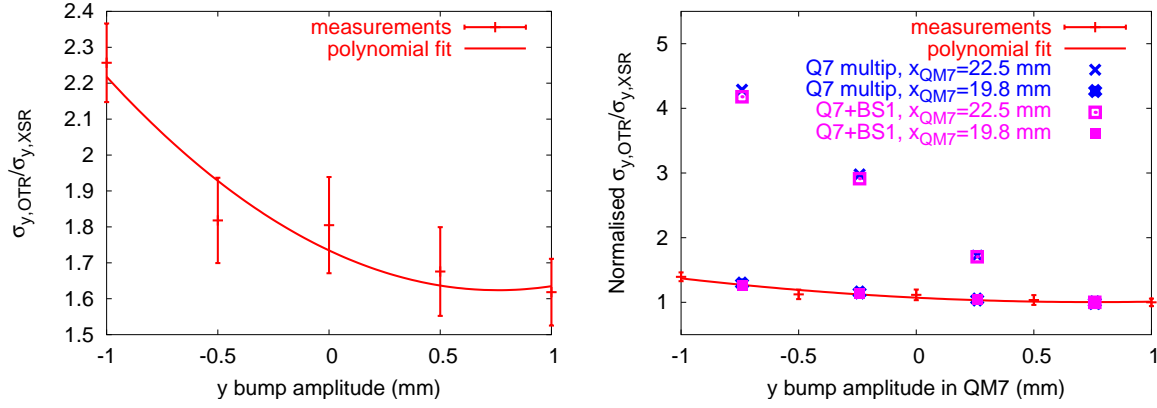
Figure 17: Ratio of vertical beam sizes at the OTR and XSR measured on the 28th of May 2008 (left) and ratio normalized to the minimum value (right), as a function of the vertical absolute bump amplitude. In the graph on the right, tracking simulation results are also shown, including the computed non-linearities in QM7R and BS1X, for the nominal horizontal orbit in QM7R (22.5 mm) and for one closer to the center of the QM7R by 2.7 mm.

6 Conclusion

Tracking simulations including the known non-linear dependances of the fields in the magnets shared by the ATF DR and extraction line were performed to determine the impact on the observed vertical emittance growth. It was found that the main effect arises from the QM7R quadrupole. The non-linearity in this magnet would have a negligible effect if the beam were always centered vertically. It can however cause significant growth of the projected vertical emittance if there is a vertical offset, because of the linear coupling induced by the sextupolar component, the main non-linear term in the multipolar field expansion of this magnet. The magnitude of the growth also depends on the horizontal displacement, increasing or decreasing in the outer and inner parts of the magnet, where the non-linearity is respectively enhanced or reduced.

An experimental program was carried out to study the dependance of the anomalous emittance growth on the extraction trajectory, by creating vertical bumps in the DR and EXT line. Beam size measurements in the DR and immediately after extracting the beam were used to infer the corresponding emittances. The results from two datasets, collected in December 2007 and at the end of May 2008, show that the growth after extraction is clearly visible but is smaller than predicted for a beam at the nominal horizontal trajectory in QM7R. The measurements can be reproduced by the simulation if one assumes horizontal displacements of a few millimeter, with the extracted beam passing through a region of QM7R nearer its center, where the non-linearity is reduced. Although the ATF orbit is usually stable at the level of about $100\,\mu$m during data taking, it could of course have offsets of several millimeters after extraction. The instrumentation available in 2007 and 2008 in the extraction line did not allow to monitor beam positions in the vicinity of QM7R and the septum magnets. Since the extraction procedure after establishing storage in the DR during initial beam setup was principally based on maximising the transmission efficiency, it could hence easily result in different offsets for each data taking period. The comparison of the measurements and simulations in December 2007 and end of May 2008 do indicate that such millimeter level horizontal offsets were likely present. Measurements including also horizontal bumps would have been very interesting to ascertain this, but there was unfortunately not enough time to perform them.

The measurements from three datasets collected in March 2008 and in the first half of May 2008 gave larger emittance values, which could not be explained by non-linear effects in the magnets considered. It is difficult to conclude anything firm from the corresponding data. On the one hand, beam sizes also varied significantly within the DR, indicating that the calculated bumps were not closed and that the beam was perhaps not sufficiently well set up for this experiment. On the other hand, the size of the extracted beam was significantly larger than expected even before implementing any bump, with magnitudes which cannot easily be explained by optical effects. Since in the current procedure to extract the beam, neither the horizontal nor the vertical trajectory can be controled or reproduced at the level of a few millimiter, one cannot exclude other types of effects arising from larger offsets in the aperture of the extraction channel.

After the measurements described in this report, the extraction line of ATF has been

reconfigured and partly rebuilt to drive the beam to the ATF2 final focus beam line. In the new design, the magnitude of the dispersion is reduced in the intial part, and the diagnostic section has larger phase advances between wire scanners, to allow more reliable emittance reconstruction. The instrumentation to monitor the positions of the extracted beam is also being significantly improved. Moreover, to mitigate effects on the projected vertical emittance from the non-linearity in the QM7R quadrupole, predicted in [4, 6, 7] and measured in this report, this magnet was replaced by another similar one with larger aperture.

Acknowledgement

References

[1] ATF2 Proposal, Vol. 1 & 2. ATF2 Collaboration, August 11 2005 and February 13 2006. `http://lcdev.kek.jp/ATF2/proposal`

[2] K. Kubo *et al.*, "Extremely low vertical-emittance beam in the Accelerator Test Facility at KEK", Phys. Rev. Lett., 88, 194801 (2002).

[3] J. Nelson, M. Ross, M. Woodley, "ATF Studies; Extraction line dispersion, beam stability and bunch length sensitivity etc", June 2000. ATF-00-06 internal report.

[4] F. Zhou, J. W. Amann, S. Seletsky, A. Seryi, C. Spencer and M. Woodley, "Simulation Studies on the Vertical Emittance Growth at the Existing ATF Extraction Beamline", Proceedings of EPAC'08, p. 652, SLAC-PUB-13279 (2008).

[5] G. Le Meur, F. Touze, "PRIAM / ANTIGONE a 2D 3D package for Accelerator Design", EPAC 94.

[6] M. Alabau Pons, A. Faus-Golfe, P. Bambade, G. Le Meur, F. Touze, "Modeling of the shared magnets of the ATF Extraction Line". CARE/ELAN Document-2008-013, ATF-08-13 Internal Report.

[7] M. Alabau Pons *et al.*, "Simulation studies on the vertical emittance growth in the ATF Extraction Line". CARE/ELAN Document-2008-014, ATF-08-14 Internal Report.

[8] C. Rimbault *et al.*, "4D Emittance Measurements using Multiple Wire and Waist Scan Methods in the ATF Extraction Line", Proceedings of EPAC'08, p. 1257, LAL-RT 08/17, ATF-08-06 internal report (2008).

[9] P. Bambade, Private Communication, March 2008.